

# Cross-Calibration Experiment of JPL AIRSAR and Truck-Mounted Polarimetric Scatterometer

Kamal Sarabandi, *Senior Member, IEEE*, Leland E. Pierce, *Member, IEEE*, Yisok Oh, *Student Member, IEEE*,  
M. Craig Dobson, *Senior Member, IEEE*, Fawwaz T. Ulaby, *Fellow, IEEE*,  
Anthony Freeman, *Member, IEEE*, and Pascale Dubois

**Abstract**—When point calibration targets are used to calibrate a SAR image, the calibration accuracy is governed by two major factors. The first factor stems from the stringent requirement on the radar cross section (RCS) of the point calibration target. To reduce the effect of radar return from the background, the RCS of a point calibration target must be much larger than that of the background. Calibration targets with large RCS require large physical dimensions for passive targets or high amplifier gain for active targets, which in practice leads to uncertainty in the nominal RCS of the targets. The second factor is related to the fact that point calibration targets are used to develop a calibration algorithm which is applied to distributed targets. To this end, accurate knowledge of the impulse response (ambiguity function) of the SAR system is required.

To evaluate the accuracy of such a calibration process, a cross-calibration experiment was conducted at a test site near Pellston, MI, using the JPL aircraft SAR and the University of Michigan truck-mounted polarimetric scatterometer. Five different types of distributed surfaces, all in the same area, were chosen: three of these were bare surfaces with varying roughnesses, and the other two were covered with vegetation (one with short grass and the other with tall grass). Trihedral corner reflectors were used for calibrating the aircraft SAR, and the UM scatterometer was calibrated using a metallic sphere. The scatterometer data were collected at  $L$  and  $C$  bands immediately after the aircraft flew over the test site.

This paper presents results of the cross calibration between the polarimetric SAR and ground-based polarimetric scatterometer measurements at  $L$  and  $C$  bands. Comparison of the data measured by the two radar systems shows that SAR calibration with trihedrals may lead to unreliable results. It is shown that coherent and incoherent interaction of the ground with a trihedral reflector can significantly alter the expected RCS of an isolated trihedral. A distributed-target calibration technique is introduced and applied to the data with good results.

## I. INTRODUCTION

CALIBRATION of polarimetric imaging radars has been the subject of intensive investigations in the past few years. The major focus has been on the removal of

the effect of radar distortions by employing well-characterized calibration targets placed in the imaged scene. Various techniques have been developed, but despite their similar goals, they differ in several ways, most notably the mathematical approach and the type and number of calibration targets used. For example, van Zyl [3] uses a trihedral corner reflector, the reciprocity of scatterers in the scene, and assumes that the co- and cross-polarized backscatter of the background are uncorrelated. In another algorithm [7], a pair of trihedral-dihedral corner reflectors plus reciprocity of the target are employed, and in the paper reported by Freeman *et al.* [6], three active radar calibrators are used. Radiometric calibration is accomplished using a known point target by integrating the power in the adjacent pixels of the point target [2] by estimating the polarimetric ambiguity function from the point target response [8].

The accuracy of an external calibration exercise depends on having accurate values for the RCS of the point targets. Each point target is designed with a large RCS in order to reduce the effect of the background. Unfortunately, the large physical dimensions of such targets introduce uncertainty into their RCS. Mutual coupling (bi-static scattering) between the calibration target and the background is another source of uncertainty. Finally, the assumptions and manipulations used in the calibration algorithm are another source of error. To evaluate the accuracy of a given calibration technique, the standard practice has been to validate the technique by measuring the RCS of a point target other than those used for calibration. This criterion reveals the accuracy of correction for channel imbalance and crosstalk. However, the real question of whether the calibration process indeed leads to accurate characterization of the response for distributed targets, such as agricultural fields or forests, has not yet been tested. To perform this test, distributed targets with known polarimetric responses are needed.

In a recent study, it was shown that the differential Mueller matrix of homogeneous distributed targets can accurately be measured by a polarimetric scatterometer using a metallic sphere as the calibration target. In the present experiment, a truck-mounted polarimetric scatterometer is used to measure the differential Mueller matrices of various types of distributed targets for the purpose of comparing them with those provided by the calibrated polarimetric SAR. By comparing the two sets of measure-

Manuscript received November 5, 1993; revised March 17, 1994. This work was supported by JPL under Contract JPL-C-95-8749.

K. Sarabandi, L. E. Pierce, M. C. Dobson, and F. T. Ulaby are with the Radiation Laboratory, Department of Electrical Engineering and Computer Science, University of Michigan, Ann Arbor, MI 48109.

Y. Oh was with the Radiation Laboratory, Department of Electrical Engineering and Computer Science, University of Michigan, Ann Arbor, MI 48109. He is now with the Department of Radio Engineering, Hong-ik University, Seoul, Korea.

A. Freeman and P. Dubois are with the Jet Propulsion Laboratory, California Institute of Technology, Pasadena, CA 91109.

IEEE Log Number 9403637.

ments, the calibration of the SAR image data can be traced to a primary standard, the metallic calibration sphere.

The details of the experimental setup are given in Section II. Data analysis and calibration are covered in Section III. The results and comparisons are presented in Section IV, followed with the conclusions in Section V.

## II. THE EXPERIMENT

To compare the backscatter data collected by the scatterometer with that measured by the SAR, appropriate homogeneous distributed targets are needed. The word "appropriate" here refers to targets with expected backscattering coefficients ( $\sigma^\circ$ ) that cover the dynamic range characteristics of natural targets. Also, the test distributed targets must be chosen such that the process by which their backscattering coefficients are measured is system independent: the correlation lengths of distributed targets must be much smaller than the footprint of the scatterometer system since this footprint is much smaller than that for the SAR system. For example, a tree canopy with trunk and branch sizes larger than the footprint of the scatterometer is not an appropriate target. Hence, only surfaces and grass-covered surfaces were selected in this purpose. Ground-truth data were collected to allow qualitative characterization of the distributed targets. Another advantage of the ground-truth data is that  $\sigma^\circ$  can be estimated using theoretical models where possible.

The experiment consists of three main parts: 1) preparation of the test fields, 2) the polarimetric SAR measurements, and 3) the truck-mounted scatterometer (POLARSCAT) measurements. The main features of each of these are covered next.

### A. Test Fields

The first step was to choose an appropriate set of distributed targets. Due to the height limitations of the truck, only short targets with relatively small correlation lengths are usable. Also, row-structured vegetation was not used in order to avoid any possible communications due to sensor orientation. Five different targets were chosen: 1) tall hay, 2) short (cut) hay, 3) very rough plowed bare soil, 4) medium-rough plowed bare soil, and 5) smooth plowed bare soil. Table I provides a summary of the target characteristics. Each field was about  $300 \times 100$  m, which corresponds to about 100 pixels in the SAR images. To reduce the effects of furrows on the backscattering, the surfaces were plowed in a  $45^\circ$  angle with respect to the flight direction. The very rough surface did not exhibit any obvious furrowing. However, the medium-rough and smooth surfaces exhibited obvious periodic furrows, although they were not taller than 10 cm. The experimental site is diagrammed in Fig. 1.

The actual surface height profiles were measured for all the surfaces using a laser profilometer with 2 mm resolution in height and steps of 1 cm over several  $1 \text{ m}^2$  areas. Also, *L*- and *C*-band dielectric probes were used to monitor the soil moisture at depths of 2 and 6 cm. Due to the lack

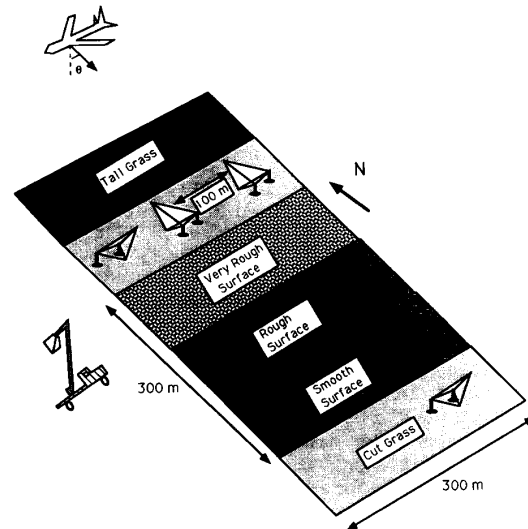


Fig. 1. Experiment site. Shown is the configuration of the three plowed fields, cut hay, and tall hay fields with the four trihedrals deployed on the cut hay.

TABLE I  
PERTINENT PHYSICAL PARAMETERS OF THE DISTRIBUTED TARGETS  
CONSIDERED IN THIS EXPERIMENT

Target	rms height	Correlation Length	Soil Moisture Cont.	
			2 cm	6 cm
Smooth Surface	0.78 cm	10.5 cm	5%	14%
Rough Surface	1.2 cm	8.95 cm	5%	14%
Very Rough Surface	4 cm	15.2 cm	5%	14%
	Height	Veg. Biomass	Veg. Moisture Cont.	
Cut Hay	5 cm	50 g/m <sup>2</sup>	70%	
Tall Hay	50 cm	667 g/m <sup>2</sup>	80%	

of precipitation over the two weeks prior to and during the experiment, both the soil moisture and roughness of the distributed targets remained constant between the SAR and truck measurements. The POLARSCAT measurements took place immediately after the SAR overflight.

### B. POLARSCAT

The University of Michigan LCS scatterometer [9] is a calibrated radar system capable of measuring the amplitude and phase of the signal backscattered from the scene illuminated by the antenna for any of the four linear polarization configurations. The system, which operates at *L* band and *C* band, and *X* band, is mounted on a truck with the antennas and RF equipment mounted on a platform at the top of a boom, and the control and processing equipment housed in a control room located on the bed of the truck. Communication between the RF units mounted on the boom and the rest of the system is accomplished via control and RF cables. The RF cables carry microwave signals sent to the RF units from the synthesizer section of the HP8753 and return samples of the backscattered signal from the RF unit to the network analyzer.

The HP8753 Vector Network Analyzer includes a microwave synthesizer that covers the range from 0.3 to 3

GHZ. The synthesizer is used as the transmit source for the *L*-band channel at 1.1–1.4 GHz. At *C*-band and *X*-band frequencies, the synthesizer output signal is up-converted to the desired frequency range by mixing it with the output of a stable Gunn oscillator, and after reception, the signal is downconverted to the same frequency of the HP8753 synthesizer.

The POLARSCAT uses dual polarized horn antennas, one for each frequency channel. This type of antenna arrangement provides excellent cross-polarization isolation over the entire main lobe, wide bandwidth, and low return loss. The POLARSCAT operates in high PRF chirped pulse mode. The high PRF pulsing enables the system to reject short range returns, including those from nearby targets, and range gating is accomplished by the time domain capability of the network analyzer.

The antennas are mounted on a rotatable positioner which allows pointing the antenna beam along any direction in azimuth or elevation (including normal incidence). Aligned with the antenna beams is a TV camera, also mounted on the positioner, used by the operator to point the antenna beam at point targets during calibration.

The truck was driven through the five fields, just after the SAR overflight, collecting data at approximately 100 points for each field at each of the three incidence angles (30°, 40°, 50°) at the same azimuth angle as the SAR (see Fig. 1).

### C. SAR

The JPL AIRSAR is fully polarimetric and transmits at *P*, *L*, and *C* bands. A typical image is in slant range format with 16-look pixels at a spacing of 12 m in azimuth and 6.66 m in slant range. Each image is approximately 12 km in azimuth and covers the range from 25° through 65° in incidence angle.

The AIRSAR flew over the fields and imaged them at three different angles (25°, 32°, 55°) which were intended to be the same as for the POLARSCAT, but an unexpected last-minute change in altitude resulted in these slightly different angles. For each intended incidence angle, a trihedral was boresighted for external calibration. Despite the shift in incidence angles, the trihedrals could still be used for calibration because they were all imaged at angles within 10° of boresight. The trihedrals used in this experiment are 2.4 m tall (leg size = 2.4 m) with nominal RCS of 33.8 and 46.8 dBsm at *L* and *C* band, respectively.

## III. DATA ANALYSIS

This section presents the important details involved in collecting, processing, and calibrating the data for each sensor. The result in each case is  $\sigma^\circ$  in dB for each field at each incidence angle, frequency, and polarization.

### A. POLARSCAT

While collecting data in the field, the truck periodically collected backscattering data from a metallic calibration

sphere at boresight. This was used later to calibrate the raw measured data. Scatterometer data calibration involves three steps. In the first step (preprocessing), the radar distortion parameters are measured over the entire main beam for each scatterometer using a calibration sphere in an anechoic chamber. The relative variation of the distortion parameters over the main beam is only a feature of the antenna system, and is independent of instabilities in the active components of the radar. The second step, measurement of the metallic sphere at boresight throughout the measurement process, is used to monitor the variations of active components between the measurement performed in the anechoic chamber and that made in the field. This also permits a periodic check of system performance. The final step is postprocessing. All the collected samples are Fourier transformed and range gated to separate the target response from the other system returns. To keep track of system drift between the calibration sphere measurement and the distributed target measurement, the response of a constant system return such as the circulator leakage in the two measurements is compared. That is, the circulator leakage which does not change with time is used as a reference between the two measurements. Fig. 2 shows the time domain responses of the calibration sphere and a distributed target, and Fig. 3 shows the variations in the circulator leakage of the *L*-band system over a 2 h period. This response was used to correct for system instability between the calibration and distributed target measurements. The reader is referred to Sarabandi *et al.* [8] for a more complete treatment of the Mueller matrix measurement and calibration process for distributed targets.

### B. JPL AIRSAR

The trihedrals deployed in the fields were used by the calibration procedure to correct the SAR image for absolute level, channel imbalance, and crosstalk, among others. POLCAL [4], the JPL calibration software, is applied to each image separately using the appropriate trihedral that had been oriented with its boresight directed at the SAR. Hence, each image is calibrated with a different trihedral.

Next, a mask is placed over that part of the image containing the test fields. For each field, the mask covers an area slightly smaller than the actual area of the field in order to eliminate the effects of interference with the responses from adjacent targets caused by the SAR impulse response (ambiguity function). Statistical averages are then performed to calculate  $\sigma^\circ$  for each region. Fig. 4 shows the *hh*-polarized power images of the fields with the field mask outlines superimposed.

Because the trihedrals were placed in the cut-hay fields, fewer pixels were available for use in the averages. This forced us to discard the data from the cut-hay fields as test targets and to exclude them in the analysis given in the next section.

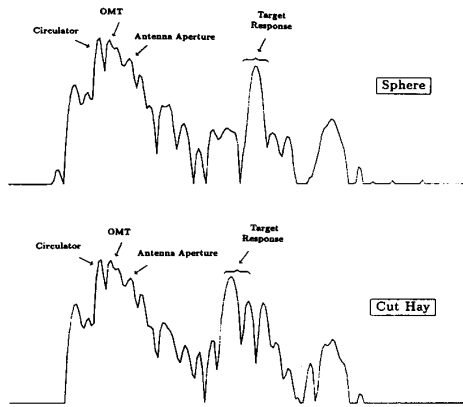


Fig. 2. Time domain response of the calibration sphere at boresight and a distributed target.

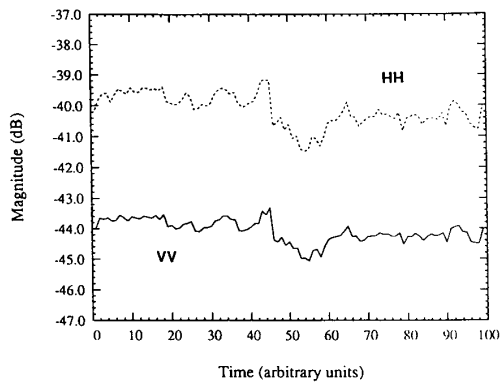


Fig. 3. The stability of  $L$ -band scatterometer over 2 h period (approximate time to collect 100 independent samples) as measured by the circular return.

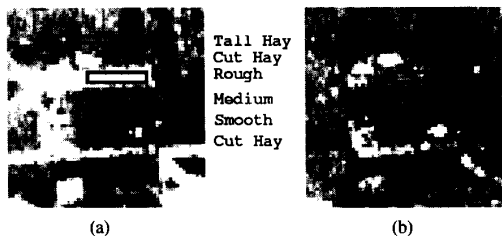


Fig. 4. SAR image. Shows an  $hh$ -polarized power JPL AIRSAR image over the test site at one of the three angles. The different fields are outlined. (a)  $L$  band, (b)  $C$  band.

#### IV. RESULTS

This section starts by presenting the POLARSCAT and AIRSAR/POLCAL data sets individually. Intercomparison of the two data sets reveals certain disagreements. The sources of discrepancy between the two data sets will be explained and removed where possible. Basically, one of the distributed targets as measured by the truck will be used as a distributed calibration target to calibrate the im-

age. An excellent agreement, in almost all cases, between the two data sets is obtained using this calibration approach.

Figs. 5 and 6 show the results of the POLARSCAT measurements at  $L$  and  $C$  band, respectively. A heuristic interpolation is applied to the POLARSCAT data, which allows the comparison with the SAR results, as the two sets of data are not at exactly the same angles. The function  $A \cos^B(\theta)$  was fit to the POLARSCAT data as the interpolation function. The POLARSCAT measurement follows the expected angular and spectral behavior for all targets. The measurement accuracy of POLARSCAT is about  $\pm 0.5$  dB for both  $L$  and  $C$  bands.

Figs. 7 and 8 show the AIRSAR/POLCAL results at  $L$  and  $C$  band, with the fit to the truck measurements for the very rough field superimposed. Two discrepancies are immediately apparent: 1) a maximum level shift of about 2 dB in  $L$  band and 4 dB in  $C$  band, and 2) angular dependence of  $\sigma^\circ$  does not fit the expected  $A \cos^B(\theta)$  for SAR. Comparison of other targets with the truck measurements of  $\sigma^\circ$  shows similar discrepancies (compare Figs. 5 and 6 to Figs. 7 and 8).

These two problems appear to be due to the use of inaccurate RCS values for the different trihedrals at the different angles in the AIRSAR images. This may be caused by two types of mechanisms: 1) ground interference effects on the measured trihedral responses, and/or 2) geometrical deformation of the trihedrals. The ground can affect the trihedral response in two ways.

1) The contribution of the background backscatter to the signal return from the trihedral and the adjacent pixels can be quite significant. This contribution not only affects the total measured power from the calibration target but also affects the polarimetric response of the trihedral, specifically,  $s_{vv}/s_{hh}$  and  $s_{hv}/s_{hh}$ , where  $s_{ij}$  is the  $ij$ -polarized scattering amplitude of the target.

2) Coherent interaction with the ground in the form of a bounce from the ground into the trihedral and vice versa, which includes both the edge diffraction and the interaction with the trihedral cavity.

Fig. 9 depicts the above-mentioned scattering interaction mechanisms. Both of these effects can increase or decrease the measured response over that which one would expect in the absence of the ground surface, depending on the phase relationship of the different contributions. To reduce the effect of the first component, the ground must be made very smooth; however, this would increase the effect of the coherent interaction component. To reduce the effect of coherent interaction, a radiowave absorber can be placed on the ground in front of the trihedral. To demonstrate the significance of this interaction of the ground with the trihedral, a number of backscatter measurements of a trihedral, both in the presence and absence of a ground plane, were conducted in an anechoic chamber at  $X$  band. Fig. 10(a) and (b) show the RCS of the trihedral as a function of elevation angle (with respect to the boresight) when the lower panel of the trihedral is making an angle of  $10^\circ$  and  $20^\circ$  with the ground plane,

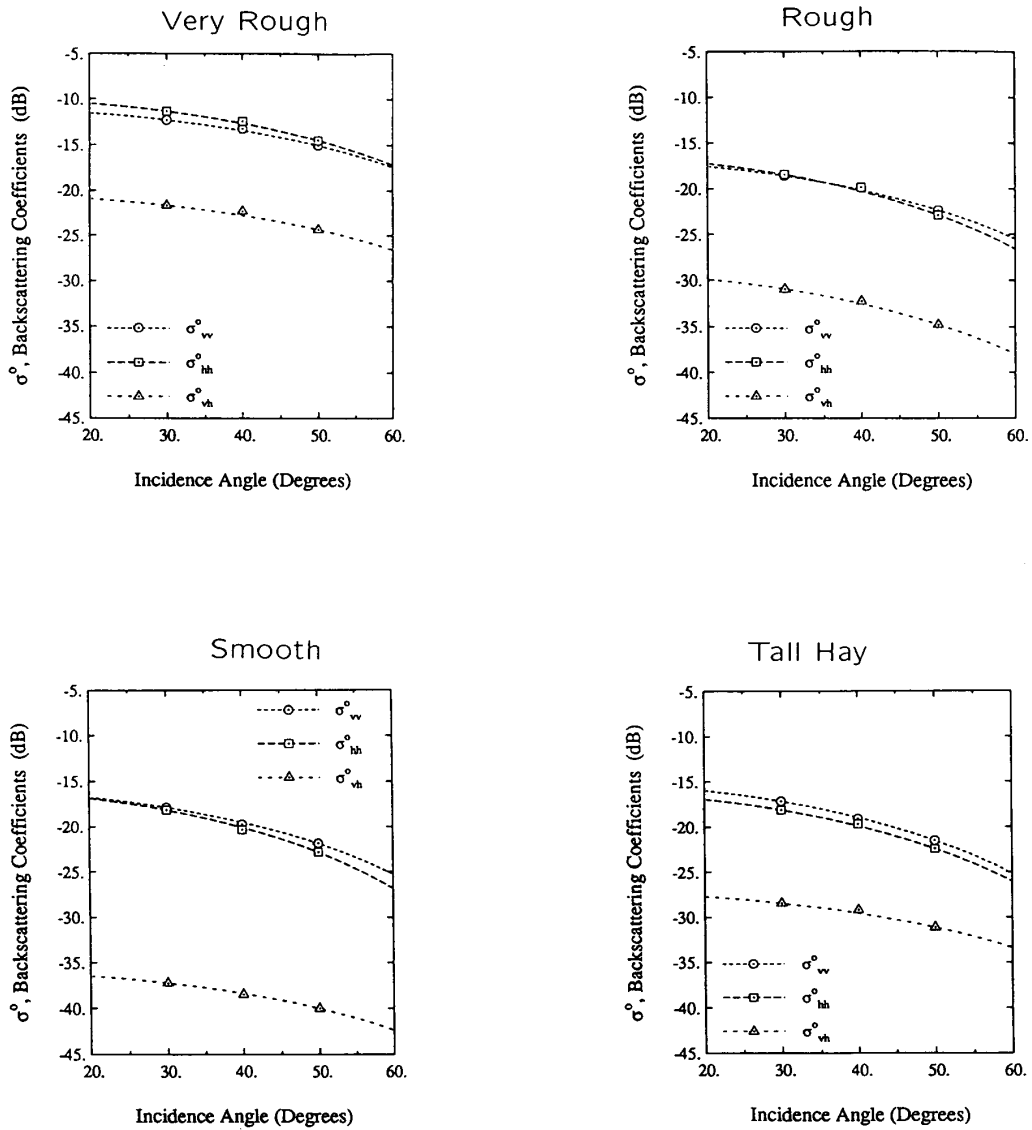


Fig. 5. POLARSCAT results. Measured backscatter from the fields using the UM POLARSCAT truck-mounted scatterometer at L band.

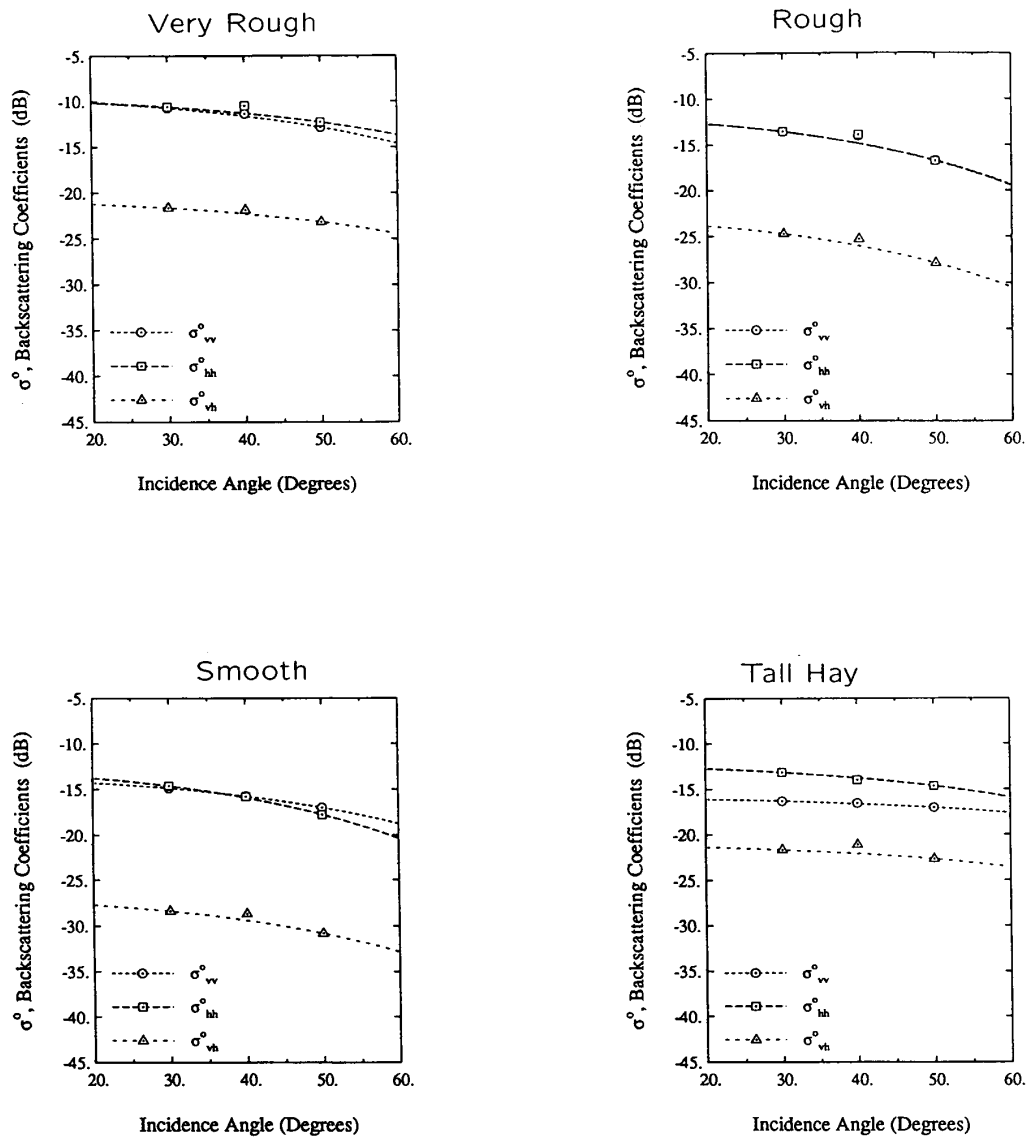


Fig. 6. POLARSCAT results. Measured backscatter from the fields using the UM POLARSCAT truck-mounted scatterometer at C band.

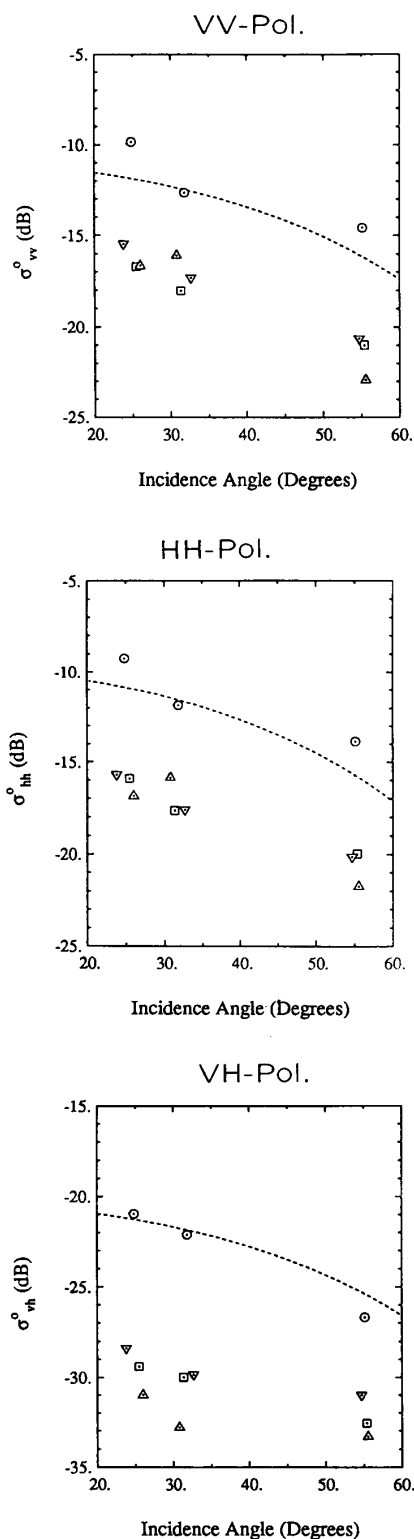


Fig. 7. AIRSAR/POLCAL results. Measured backscatter from the fields using the JPL AIRSAR and POLCAL calibration software at *L* band in conjunction with trihedral reflectors; (---) truck for very rough, (○) very rough, (□) rough, (△) smooth, (▽) tall hay.

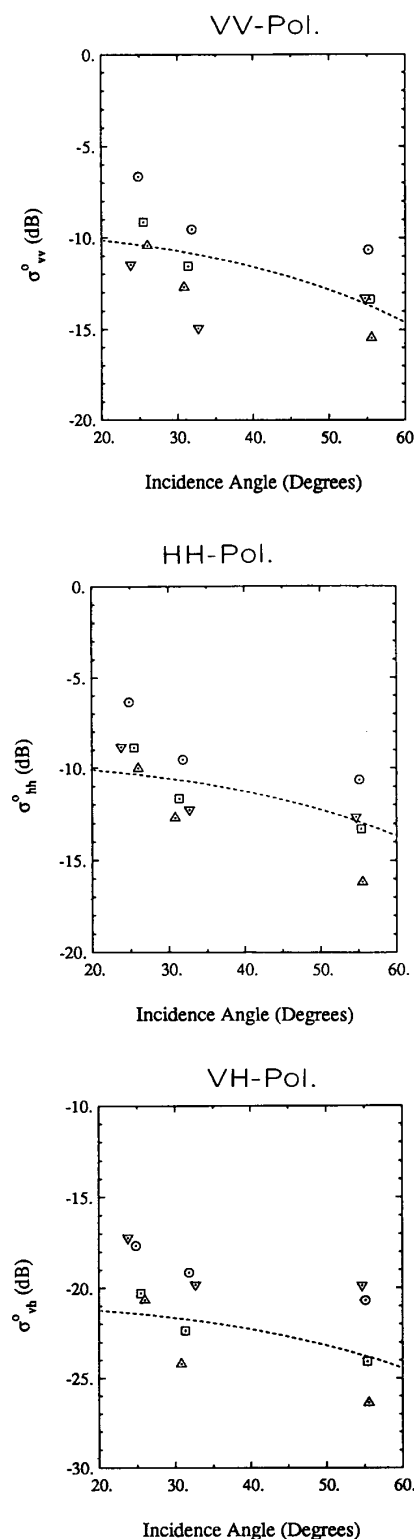


Fig. 8. AIRSAR/POLCAL results. Measured backscatter from the fields using the JPL AIRSAR and POLCAL calibration software at *C* band in conjunction with trihedral reflectors; (---) truck for very rough, (○) very rough, (□) rough, (△) smooth, (▽) tall hay.

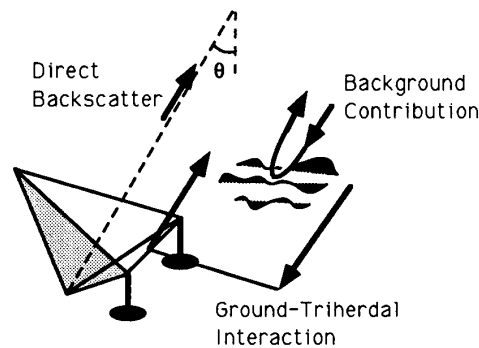


Fig. 9. Effect of ground on trihedral responses. RCS of an isolated trihedral is affected by direct background contribution and ground-trihedral interaction.

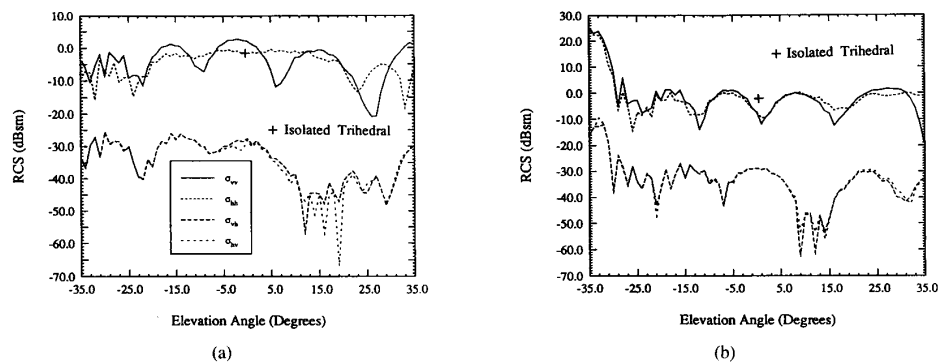


Fig. 10. Measured RCS elevation pattern of a trihedral with  $l = 4\lambda$  above a ground plane at 9.5 GHz. The angle between the lower panel and the ground is: (a)  $10^\circ$ , (b)  $20^\circ$ .

respectively. It is shown that the RCS scattering pattern and the ratio of copolarized components of the trihedral in the presence of the ground plane have significantly changed.

The geometrical deformation of the trihedrals can be in the form of warped panels or nonperpendicular sides. Both would cause a decrease in the measured response of the trihedral [5].

All of these problems were observed to occur for some of the trihedrals used in this experiment, but since no quantitative method exists for correcting for them, no corrections of this kind can be attempted.

To circumvent the calibration problems caused by the background contribution and the possible geometrical deformation, one of the distributed targets with known backscatter coefficient was used as the calibration target. We chose the very rough field as the distributed calibration target, as that has the highest signal-to-noise ratio. In this approach, since the backscattering coefficients are being compared directly, the need for knowledge of the ambiguity function is eliminated. The results of this calibration approach are shown in Figs. 11 and 12 for  $L$  and  $C$  band, respectively, where each of the remaining fields

is plotted as single points, with the perfect agreement line being the diagonal through each plot. The errors in the copolarized responses are now quite low, mostly less than 1 dB, while the cross-polarized response has large errors when the measured level is below  $-30$  dB. This error in the cross-polarized response appears to be due to the inability of POLCAL to remove crosstalk below this level.

There are still two fields that show poor agreement: 1) smooth,  $32^\circ$ ,  $L$  band; and 2) medium rough,  $55^\circ$ ,  $C$  band. This may be due to the Bragg diffraction from the slight furrow structure that remained after the roughening/smoothing phase, which was necessarily carried out with standard farming tools. In particular, the smooth field had an average furrow spacing  $L = 16.5$  cm, with furrows at  $45^\circ$  to the SAR look direction. For Bragg diffraction, it is required that  $\sin \theta = m\lambda/L$ . For  $L = 2\sqrt{2} \times 16.5$  cm,  $\lambda = 25$  cm, and  $m = 1$ , the Bragg equation gives  $\theta = 31^\circ$ , very near the  $32^\circ$  angle at which the measurement took place. A similar calculation can be performed for the medium rough surface at  $C$  band:  $L = 2\sqrt{2} \times 31.5$  cm,  $\lambda = 5.66$  cm, and  $m = 13$ , which gives  $\theta = 55.5^\circ$ , very near the actual  $55^\circ$  of the SAR measurement. Hence, these two outliers can be ignored in the comparisons.



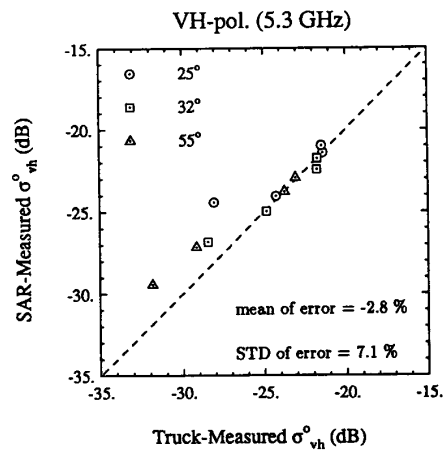
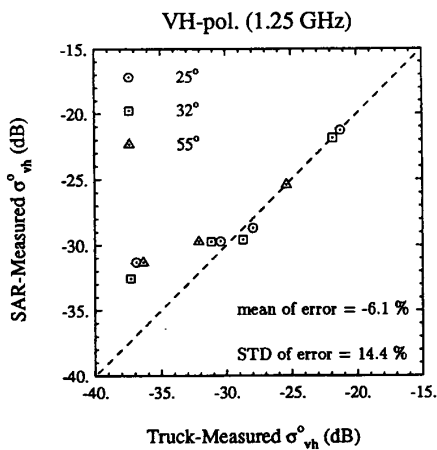
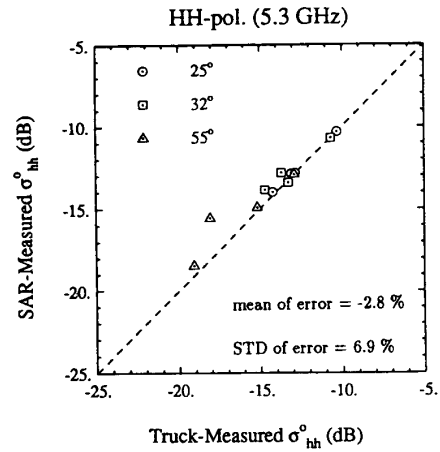
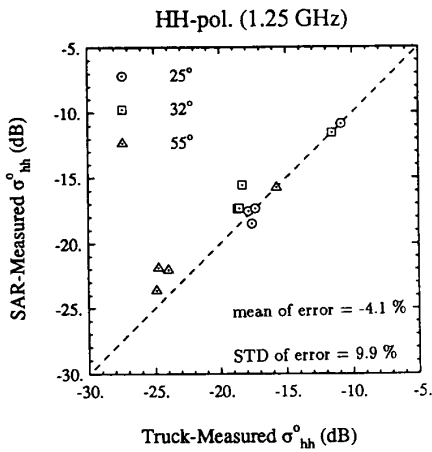
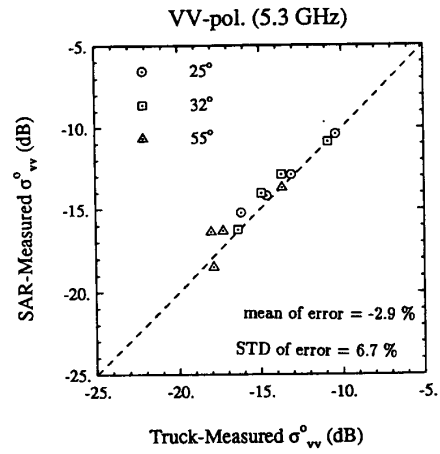
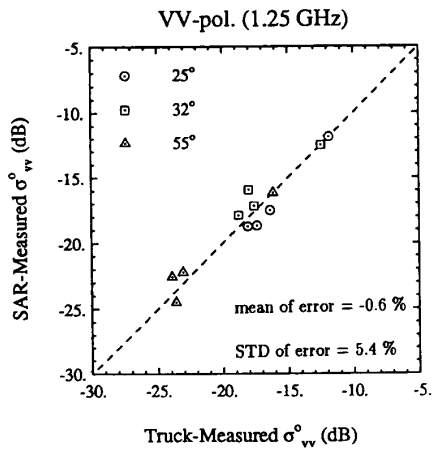


Fig. 11. Comparison of POLARSCAT with AIRSAR corrected data. The JPL AIRSAR data have been calibrated using the POLARSCAT data for the very rough field. The data for the remaining fields are plotted at L band.

Fig. 12. Comparison of POLARSCAT with AIRSAR corrected data. The JPL AIRSAR data have been calibrated using the POLARSCAT data for the very rough field. The data for the remaining fields are plotted at C band.

## V. CONCLUSIONS

External calibration of polarimetric SAR using point targets is examined by comparing the calibrated SAR backscattering with those measured by a calibrated scatterometer system. It is shown that calibration using a point target is rather unreliable. A maximum discrepancy of 3 dB for *L* band and 5 dB for *C* band between the SAR and scatterometer measurements was observed. The interactions with the ground and the uncertainties in the trihedral shape are mostly responsible for the errors in the SAR data. A large number of trihedrals may help in removing the ground contribution through an averaging process, but only careful handling and exacting standards during field assembly can mitigate the geometrical problems: an arduous task at best.

The heuristic interpolation applied to the SAR data, using the roughest field as a calibration target, implies that SAR calibration using distributed targets may be the most reliable solution. With the calibration approach using the roughest surface as the calibration target, a maximum deviation of about 1 dB was observed in the copolarized channels and in the cross-polarized channels when  $\sigma^\circ > -30$  dB. The error was larger for smaller values of cross-polarized response because of the inability of POLCAL to remove the crosstalk effectivity. This crude calibration using a distributed target suggests that known distributed targets may be a better alternative for external calibration of imaging radars.

## ACKNOWLEDGMENT

The authors appreciate the help for the JPL Radar Science group in providing the POLCAL software and the AIRSAR image data used in this study.

## REFERENCES

- [1] K. Sarabandi, L. E. Pierce, and F. T. Ulaby, "Calibration of a polarimetric imaging SAR," *IEEE Trans. Geosci. Remote Sensing*, vol. 30, p. 540, May 1992.
- [2] A. L. Gray, P. W. Vachon, C. E. Livingstone, and T. I. Lukowski, "Synthetic aperture radar calibration using reference reflectors," *IEEE Trans. Geosci. Remote Sensing*, vol. 28, p. 374, May 1990.
- [3] J. J. van Zyl, "Calibration of polarimetric radar images using only image parameters and trihedral corner reflector responses," *IEEE Trans. Geosci. Remote Sensing*, vol. 28, p. 337, May 1990.
- [4] J. J. van Zyl, C. F. Burnette, H. A. Zebker, A. Freeman, and J. Holt, *POLCAL User's Manual*, Jet Propulsion Lab., Aug. 1990.
- [5] D. Kahny and J. J. van Zyl, "How does corner reflector construction affect polarimetric SAR calibration?," in *Proc. Int. Geosci. Remote Sensing Symp. '90 (IGARSS '90)*, vol. 2, 1990, p. 1093.
- [6] A. Freeman, Y. Chen, and C. L. Werner, "Polarimetric SAR calibration experiment using active radar calibrators," *IEEE Trans. Geosci. Remote Sensing*, vol. 28, p. 224, Mar. 1990.
- [7] J. D. Klein and A. Freeman, "Quandpolarization SAR calibration using target reciprocity," *J. Electromag. Waves and Appl.*, vol. 5, no. 7, p. 735, 1991.
- [8] K. Sarabandi, Y. Oh, and F. T. Ulaby, "Measurement and calibration of differential Mueller matrix of distributed targets," *IEEE Trans. Antennas Propagat.*, vol. 40, Dec. 1992.
- [9] M. A. Tassoudji, K. Sarabandi, and F. T. Ulaby, "Design consideration and implementation of the LCX polarimetric scatterometer (POLARSCAT)," Radiation Laboratory Report No. 022486-T-2, June 1989.



**Kamal Sarabandi** (S'87-M'90-SM'93) received the B.S. degree in electrical engineering from Sharif University of Technology, Tehran, Iran, in 1980. He entered the graduate program at the University of Michigan in 1984 and received the M.S.E. degree in electrical engineering in 1986, the M.S. degree in mathematics, and the Ph.D. degree in electrical engineering in 1989.

From 1980 to 1984 he worked as a Microwave Engineer at the Telecommunication Research Center, Iran. He is presently an Assistant Professor in the Department of Electrical Engineering and Computer Science at the University of Michigan. His research interests include electromagnetic scattering, microwave and millimeter wave remote sensing, computational electromagnetics, and calibration of polarimetric SAR systems.

Dr. Sarabandi is the elected Chairman of the IEEE Geoscience and Remote Sensing Society Michigan Chapter, and a member of the Electromagnetics Academy and USNC/URSI Commission F.



**Leland E. Pierce** (S'85-M'85-M'89) received the B.S. degrees in both electrical and aerospace engineering in 1983, and the M.S. and Ph.D. degrees in electrical engineering in 1986 and 1991, respectively, all from the University of Michigan, Ann Arbor.

Since then, he has been the Head of the Microwave Image Processing Facility within the Radiation Laboratory in the Electrical Engineering and Computer Science Department at the University of Michigan, Ann Arbor, where he is responsible

for research into the uses of polarimetric SAR systems for remote sensing applications, specifically, forest canopy parameter inversion.

**Yisok Oh** (S'88) received the B.S. degree from Yonsei University, Seoul, Korea, in 1982, the M.S. degree from the University of Missouri, Rolla, in 1988, and the Ph.D. degree from the University of Michigan, Ann Arbor, in 1993, all in electrical engineering.

He is presently an Assistant Professor in the Department of Radio Engineering at the Hong IK University. His research interests include electromagnetic wave scattering from random surfaces and microwave remote sensing.



**M. Craig Dobson** (M'80-SM'91) received the B.A. degrees in geology and anthropology from the University of Pennsylvania, Philadelphia, in 1973, and the M.A. degree in geography from the University of Kansas, Lawrence, in 1981.

At the Remote Sensing Laboratory of the University of Kansas Center for Research, Inc. (1975-1984), he managed several experimental programs related to microwave remote sensing of terrain. Specific research projects focused on the microwave dielectric properties of soils, microwave sensor response to soil moisture and crop canopy cover using truck-mounted and airborne scatterometers and radiometers, and multitemporal simulations of orbital SAR imagery. Since 1984, he has been with the Radiation Laboratory of the Electrical Engineering and Computer Science Department of the University of Michigan, where he is now an Associate Research Scientist, conducting research on the microwave dielectric properties of vegetation and radar backscattering properties of forests.



**Fawwaz T. Ulaby** received the B.S. degree in physics from the American University of Beirut, Lebanon, in 1964 and the M.S.E.E. and Ph.D. degrees in electrical engineering from the University of Texas, Austin, in 1966 and 1968, respectively.

He is the R. Jamison and Betty Williams Professor of Electrical Engineering and Computer Science at the University of Michigan, Ann Arbor, and Director of the NASA Center for Space Terahertz Technology. His current interests include

microwave and millimeter wave remote sensing, radar systems, and radio wave propagation. He has authored eight books and published over 400 papers and reports on these subjects.

Dr. Ulaby is the recipient of numerous awards, including the Eta Kappa Nu Association C. Holmes MacDonalld Award as "An Outstanding Electrical Engineering Professor in the United States of America for 1975," the IEEE Geoscience and Remote Sensing Distinguished Achievement Award (1983), the IEEE Centennial Medal (1984), the American Society of Photogrammetry's Presidential Citation for Meritorious Science (1984), the Kuwait Prize in Applied Science (1986), NASA Group Achievement Award (1990), and the University of Michigan Distinguished Faculty Achievement Award (1991). He served as President of the IEEE Geoscience and Remote Sensing Society (1980-1982), as Executive Editor for its *TRANSACTIONS* (1983-1985), and as General Chairman of several international symposia. He is a member of URSI Commission F and serves on several scientific boards and professional committees.



**Anthony Freeman** (M'83) received the B.Sc. (Hons.) degree in mathematics in 1979 and the Ph.D. degree in astrophysics in 1982, both from the University of Manchester Institute of Science and Technology, Manchester, England.

Between 1982 and 1987 he worked at the Marconi Research Centre, Chelmsford, England, on moving target imaging with SAR, aircraft SAR motion compensation, SAR design studies, and image quality assessment. Since March 1987 he has been employed by the Jet Propulsion Labo-

ratory, California Institute of Technology, Pasadena, as a Radar Systems Specialist and Group Supervisor. His group is responsible for calibration of the SIR-C data products and studies of advanced radar systems. His current research interests are in the field of multifrequency, multipolarization SAR calibration and in classification and information extraction from SAR imagery.

Dr. Freeman is Chairman of the Committee on Earth Observing Sensors (CEOS) Working Group on SAR calibration. He is a principal investigator on three NASA-sponsored studies: one on SIR-C calibration, one on calibration and change detection using Alaska SAR Facility ERS-1 data, and one on geographical information systems.

**Pascale Dubois** received the *diplome d'ingenieur* from the Ecole Nationale Supérieure d'Ingenieur en Construction Aeronautique, Toulouse, France in 1982, and the M.S. and Engineer's degree from the California Institute of Technology, Pasadena, in 1983 and 1985, respectively.

She is currently working at the Jet Propulsion Laboratory, Pasadena, CA, in the Radar Science and Technology Section. Her research interest includes scattering from rough surfaces, polarimetry, and the applications of remote sensing to hydrology and geology.